

# Structural basis for m<sub>3</sub>G-cap-mediated nuclear import of spliceosomal UsnRNPs by snurportin1

Anja Strasser<sup>1</sup>, Achim Dickmanns<sup>1</sup>,  
Reinhard Lührmann<sup>2</sup> and Ralf Ficner<sup>1,\*</sup>

<sup>1</sup>Department of Molecular Structural Biology, Institute for Microbiology and Genetics, University Göttingen, Germany and <sup>2</sup>Department of Cellular Biochemistry, Max-Planck-Institute of Biophysical Chemistry, Göttingen, Germany

In higher eukaryotes the biogenesis of spliceosomal UsnRNPs involves a nucleocytoplasmic shuttling cycle. After the m<sup>7</sup>G-cap-dependent export of the snRNAs U1, U2, U4 and U5 to the cytoplasm, each of these snRNAs associates with seven Sm proteins. Subsequently, the m<sup>7</sup>G-cap is hypermethylated to the 2,2,7-trimethylguanosine (m<sub>3</sub>G)-cap. The import adaptor snurportin1 recognises the m<sub>3</sub>G-cap and facilitates the nuclear import of the UsnRNPs by binding to importin-β. Here we report the crystal structure of the m<sub>3</sub>G-cap-binding domain of snurportin1 with bound m<sub>3</sub>GpppG at 2.4 Å resolution, revealing a structural similarity to the mRNA-guanylyltransferase. Snurportin1 binds both the hypermethylated cap and the first nucleotide of the RNA in a stacked conformation. This binding mode differs significantly from that of the m<sup>7</sup>G-cap-binding proteins Cap-binding protein 20 (CBP20), eukaryotic initiation factor 4E (eIF4E) and viral protein 39 (VP39). The specificity of the m<sub>3</sub>G-cap recognition by snurportin1 was evaluated by fluorescence spectroscopy, demonstrating the importance of a highly solvent exposed tryptophan for the discrimination of m<sup>7</sup>G-capped RNAs. The critical role of this tryptophan and as well of a tryptophan continuing the RNA base stack was confirmed by nuclear import assays and cap-binding activity tests using several snurportin1 mutants.

*The EMBO Journal* (2005) 24, 2235–2243. doi:10.1038/sj.emboj.7600701; Published online 26 May 2005

**Subject Categories:** structural biology; RNA

**Keywords:** 5'-cap; crystallography; nuclear transport; snurportin1; UsnRNP

## Introduction

The transport of macromolecules between the nuclear and cytoplasmic compartments in eukaryotic cells is achieved by transport factors, most of them belonging to the importin-β superfamily (Görlich and Kutay, 1999; Chook and Blobel, 2001; Weis, 2003). Nuclear import of karyophilic proteins

bearing a canonical nuclear localisation signal (NLS) requires the recognition by the adaptor importin-α, which in turn binds to importin-β via an N-terminal importin-β-binding (IBB) domain (Görlich *et al.*, 1996). The interaction with and translocation through the nuclear pore complex is mediated by importin-β. Besides the importin-α/β-dependent nuclear import, several alternative pathways have been identified (Görlich and Kutay, 1999; Weis, 2003). Among these pathways, there is an exceptional strategy that has evolved in higher eukaryotes for the transport of spliceosomal UsnRNPs, namely U1, U2, U4 and U5, as their biogenesis involves a nucleocytoplasmic shuttling cycle (Will and Lührmann, 2001).

Transcription and modification of the 3' and 5' ends leads to m<sup>7</sup>G-capped UsnRNAs that are recognised by the cap-binding proteins Cap-binding protein 20 (CBP20)/80. Three additional proteins, phosphorylated adaptor for RNA export (PHAX), the actual export receptor chromosome region maintenance 1 (CRM1) or Exportin1 (Xpo1; Ohno *et al.*, 2000) and Ras-related nuclear antigen (RanGTP; Ohno *et al.*, 2000; Segref *et al.*, 2001) are required for the export of the UsnRNAs into the cytoplasm.

In the cytoplasm, seven Sm proteins bind to the Sm site common to these UsnRNAs, forming the snRNP core complex. This assembly process is mediated by the SMN complex (Meister *et al.*, 2002; Gubitz *et al.*, 2004; Yong *et al.*, 2004). Proper assembly of the core UsnRNPs and the SMN complex bound to it is a prerequisite for the hypermethylation of the m<sup>7</sup>G-cap to the 2,2,7-trimethyl-guanosine (m<sub>3</sub>G)-cap (Mattaj, 1986; Massenet *et al.*, 2002). Initial studies on the cap hypermethylation of human U1snRNP showed that the snRNA-(guanosine-N<sup>2</sup>)-methyltransferase is an S-adenosyl-methionine-dependent enzyme that binds to the SmB/B' proteins (Plessel *et al.*, 1994). Further *in vitro* reconstitution experiments revealed that the presence of the SmB/B' protein in the snRNP core complex is essential for the cap hypermethylation (Raker *et al.*, 1996). Finally, the cap hypermethylase was identified in *Saccharomyces cerevisiae* and denoted TGS1 (for Trimethyl-Guanosine Synthase) (Mouaikel *et al.*, 2002). A sequence database search revealed that the putative mammalian orthologs are significantly larger, with their C-terminal domain harbouring the conserved methyltransferase domain (Mouaikel *et al.*, 2002).

The m<sub>3</sub>G-cap is part of a bipartite NLS specific for UsnRNP nuclear import (Fischer and Lührmann, 1990; Fischer *et al.*, 1991). The second signal is located on the Sm-core RNP complex (Fischer *et al.*, 1993). The functionality of both import signals has been shown to depend on importin-β (Palacios *et al.*, 1997; Huber *et al.*, 1998; Narayanan *et al.*, 2004). The m<sub>3</sub>G-cap is specifically recognised by snurportin1, which acts as an adaptor between the UsnRNP cargo and importin-β (Huber *et al.*, 1998). Snurportin1 consists of two functional domains, the N-terminal IBB domain and the m<sub>3</sub>G-cap-binding domain. The IBB domain comprises amino acids 1–65 and exhibits high homology to the IBB domains of other

\*Corresponding author. Abt. Molekular Strukturbiologie, Institut für Mikrobiologie und Genetik, Universität Göttingen, Justus-von-Liebig-Weg 11, 37077 Göttingen, Germany. Tel.: +49 551 39 14071; Fax: +49 551 39 14082; E-mail: rficner@gwdg.de

Received: 27 January 2005; accepted: 9 May 2005; published online: 26 May 2005

transport adaptors, such as importin- $\alpha$  and RIP- $\alpha$ , that use importin- $\beta$  as a transport receptor (Görllich *et al*, 1996; Jullien *et al*, 1999; Huber *et al*, 2002). The m<sub>3</sub>G-cap-binding domain, ranging from amino acids 95 to 300, shares no significant sequence similarities with other cap-binding proteins or with any other protein (Huber *et al*, 1998).

The three-dimensional structures of several m<sup>7</sup>G-cap-binding proteins, namely CBP20 of the cap-binding complex (CBC) involved in nuclear export of UsnRNA (Calero *et al*, 2002; Mazza *et al*, 2002), the viral nucleoside 2'-O-methyltransferase VP39 (Hodel *et al*, 1997, 1998; Hu *et al*, 2002) and the eukaryotic translation initiation factor 4E (eIF4E) (Marcotrigiano *et al*, 1997; Matsuo *et al*, 1997; Niedzwiecka *et al*, 2002; Tomoo *et al*, 2003) have been determined. Despite the lack of structural similarity, they all reveal a common strategy in the specific binding of m<sup>7</sup>G-cap-bearing RNAs. These proteins interact with the m<sup>7</sup>G-cap by sandwiching the monomethylated guanine base between two aromatic side chains. However, to date there has been no experimental clue as to whether snurportin1 shares that canonical binding mode of the m<sup>7</sup>G-cap-binding proteins, or whether a different strategy is used for specific binding of the m<sub>3</sub>G-cap. Hence, the crystal structure determination of snurportin1 in complex with m<sub>3</sub>G-cap has been of particular interest in order to reveal and understand the structural basis for the specific recognition of the m<sub>3</sub>G-cap by snurportin1. After all attempts to crystallise full-length snurportin1 either by itself or in complex with m<sub>3</sub>G-cap oligo and/or importin- $\beta$  had failed, we focused on the structure determination of the m<sub>3</sub>G-cap-binding domain of human snurportin1 identified by limited proteolysis experiments (Strasser *et al*, 2004). Although a 37 kDa fragment of snurportin1 was used for crystallisation, the obtained single crystals contain just a 26 kDa m<sub>3</sub>G-cap-binding fragment, indicating a continuation of proteolysis within the crystallisation droplet (Strasser *et al*, 2004).

We have determined the crystal structure of the 26 kDa m<sub>3</sub>G-cap-binding domain of human snurportin1 in complex with an m<sub>3</sub>G-cap dinucleotide. Snurportin1 binds the m<sub>3</sub>G-base and the first base of the UsnRNA in a stacked conformation. This is in contrast to the structurally characterised m<sup>7</sup>G-cap-binding proteins, where only the cap base is sandwiched between two aromatic side chains. In order to investigate this novel binding mode in more detail, binding constants of several cap oligonucleotides to snurportin1 were determined by fluorescence spectroscopy, and the role of the tryptophan residues in the binding pocket was analysed by nuclear import assays and spectroscopic cap-binding affinity tests for various tryptophan mutants.

## Results and discussion

### Structure of the snurportin1-m<sub>3</sub>G-cap complex

The crystal structure of the m<sub>3</sub>G-cap-binding domain of human snurportin1 was determined by means of MIRAS using several heavy-atom derivatives and refined at a resolution of 2.4 Å (Table I). The overall structure is composed of five  $\alpha$ -helices and 10  $\beta$ -strands that form two almost coplanar  $\beta$ -sheets linked by two crossing  $\beta$ -strands (Figure 1). The m<sub>3</sub>G-cap-binding pocket is located between the two  $\beta$ -sheets; several residues of strands  $\beta$ 1,  $\beta$ 3,  $\beta$ 10 and adjacent loop regions interact with the entire m<sub>3</sub>G-cap dinucleotide (Figure 2A, see Supplementary Figure 1). Both bases of the

bound m<sub>3</sub>GpppG are in a nearly coplanar orientation 3.5–3.8 Å apart, but slightly displaced with respect to a perfect base stacking (Figure 2B). The six-membered ring of the nonmethylated guanine is almost perfectly centered on the dimethylated N2 atom (Figure 2B). The base-stacking of the dinucleotide is continued by the side chain of Trp276 on the side of the trimethylated guanine, and is flanked by Leu104 on the side of the nonmethylated guanine (Figure 2A). Additionally, the m<sub>3</sub>G-base is in hydrophobic contact with the side chains of Glu106 and Trp107, the latter in an almost perpendicular orientation to the stack with a distance of 4.3 Å. Remarkably, the protein forms only two hydrogen bonds with the trimethylated guanine base. The hydroxyl group of Ser105 donates a hydrogen to O6 and accepts one from N1 (Figure 2A). The nonmethylated guanine also forms hydrogen bonds with Ser105 as its NH<sub>2</sub> group at position 2, N1 is hydrogen-bonded to the main-chain carbonyl oxygen, and O6 accepts the hydrogen of the main-chain amide. The interaction is further stabilised by hydrogen bonds between several basic residues, the triphosphate and the riboses. The side chain of Lys128 and the main-chain amide of Arg129 interact with phosphate oxygens, and Lys144 is in contact with the cyclic oxygen of the ribose of the first snRNA nucleotide, as well as with phosphate oxygens (Figure 2A, see Supplementary Figure 1). A database search revealed that all residues involved in the interaction with the m<sub>3</sub>GpppG dinucleotide are highly conserved among all known snurportin1 sequences. The only exception was found in *Arabidopsis thaliana*, where Ser105 is replaced by a proline residue. This replacement is structurally possible, but appears very unlikely due to the loss of hydrogen bonds involved in ligand binding. Since only a single base exchange is necessary to change serine into proline, an error of the database entry could also be plausible.

The binding mode of the m<sub>3</sub>G-cap by snurportin1 differs significantly from that observed for the m<sup>7</sup>G-cap-binding proteins CBP20, eIF4E and VP39, as these proteins always intercalate the m<sup>7</sup>G-base between two aromatic side chains and keep the bound di- or oligonucleotides in an extended conformation (Figure 3) (Hodel *et al*, 1997, 1998; Calero *et al*, 2002; Mazza *et al*, 2002; Niedzwiecka *et al*, 2002; Tomoo *et al*, 2003).

So far only crystals of the m<sub>3</sub>G-cap-binding domain with bound m<sub>3</sub>GpppG have been obtained. All attempts to crystallise full-length snurportin1 have failed, probably due to a high degree of conformational flexibility between the N-terminal IBB domain and the m<sub>3</sub>G-cap-binding domain. Also, no crystals of the m<sub>3</sub>G-cap-binding domain could be obtained in the absence of m<sub>3</sub>GpppG, indicating an effect of the dinucleotide on the structural integrity of the protein. Furthermore, it was not possible to crystallise a complex using a larger oligonucleotide, like synthetic m<sub>3</sub>GpppA<sub>m</sub>pU<sub>m</sub>pA, which resembles the UsnRNAs more closely. The inspection of the crystal packing revealed that a larger cap oligonucleotide could not be accommodated in this crystal form of the snurportin1-m<sub>3</sub>GpppG complex.

### Mode of interaction between snurportin1 and m<sub>3</sub>G-cap

During UsnRNP biogenesis, the hypermethylation of the m<sup>7</sup>G-cap occurs after assembly of the Sm-core UsnRNP complex and initiates the import of this complex into the nucleus. Therefore, the specificity of m<sub>3</sub>G-cap binding by snurportin1

**Table I** Crystallographic data and refinement statistics

Data collection Data set	Native	MIRAS		
		Hg	U	Pt
Wavelength (Å)	0.98	1.54	1.54	1.54
Resolution range (Å)	20–2.4 (2.5–2.4)	100–3.5 (3.6–3.5)	100–3.5 (3.6–3.5)	100–3.5 (3.6–3.5)
Space group	P4 <sub>1</sub> 2 <sub>1</sub> 2	P4 <sub>1</sub> 2 <sub>1</sub> 2	P4 <sub>1</sub> 2 <sub>1</sub> 2	P4 <sub>1</sub> 2 <sub>1</sub> 2
Cell dimensions (Å)	<i>a</i> = <i>b</i> = 57.47 <i>c</i> = 130.09	<i>a</i> = <i>b</i> = 57.43 <i>c</i> = 130.83	<i>a</i> = <i>b</i> = 57.09 <i>c</i> = 130.5	<i>a</i> = <i>b</i> = 57.12 <i>c</i> = 131.47
No. of reflections	24 9994 (8674)	57 589 (3113)	54 724 (2993)	109 333 (3087)
Completeness (%)	95.4 (66.3)	100.0 (100.0)	97.5 (99.3)	99.7 (100.0)
Average <i>I</i> /δ	18.7 (3.0)	18.1 (9.3)	11.7 (4.6)	16.2 (3.6)
<i>R</i> <sub>merge</sub>	0.09 (0.25)	0.112 (0.3)	0.124 (0.27)	0.132 (0.55)
<b>MIRAS phasing</b>				
Heavy-atom sites		4	3	4
Phasing power				
Isomorphous		1.631	1.005	0.782
Anomalous		0.627	0.845	0.312
<i>R</i> -cullis				
Isomorphous		0.644	0.799	0.834
Anomalous		0.922	0.914	0.976
Overall figure of merit				
Before solvent flattening	0.23			
After solvent flattening	0.75			
<b>Refinement statistics</b>				
<i>R</i> -factor (%)	22.7 (32.1)			
<i>R</i> <sub>free</sub> (%)	27.6 (40.3)			
No. of protein atoms	1604			
No. of ligand atoms	53			
No. of water molecules	77			
Ramachandran plot statistics				
Most favourable regions (%)	87.6			
Additionally allowed regions (%)	11.2			
Generously allowed regions (%)	1.2			
Disallowed regions (%)	0.0			
r.m.s. deviations from ideal values				
Bond distances (Å)	0.0074			
Angles (deg)	1.75			
Average <i>B</i> -value protein (Å <sup>2</sup> )	46.7			
Average <i>B</i> -value m <sub>3</sub> GpppG (Å <sup>2</sup> )	75.5			

Values in parenthesis refer to the highest resolution shells.

$R_{\text{merge}} = \frac{\sum_{hkl} \sum_i |I_i(hkl) - \langle I_i(hkl) \rangle|}{\sum_{hkl} \sum_i \langle I_i(hkl) \rangle}$ , where the sum *i* is over all separate measurements of the unique reflection *hkl*.

$R\text{-factor} = \frac{\sum_{hkl} |F_{\text{obs}} - F_{\text{calc}}|}{\sum_{hkl} F_{\text{obs}}}$ .

*R*<sub>free</sub> as *R*-factor, but summed over a 5% test set of reflections.

is of particular interest with respect to the discrimination of m<sup>7</sup>G-cap-bearing UsnRNAs and mRNAs, preventing their accidental reimport into the nucleus. The physiological cargoes of human snurportin1 share the common sequence m<sub>3</sub>GpppA<sub>m</sub> at the 5′ end of the UsnRNA. Previous studies have already demonstrated that an m<sub>3</sub>GpppG dinucleotide is sufficient to be bound by snurportin1, and that the binding of m<sup>7</sup>GpppG to snurportin1 is two to three orders of magnitude less efficient than that of m<sub>3</sub>GpppG (Huber *et al.*, 1998). In order to quantify the interaction of snurportin1 with different 5′-caps, we determined the binding constants of various 5′-oligonucleotides by means of fluorescence spectroscopy (Table II). For these experiments the full-length snurportin1 was used, as the crystallised 26 kDa domain formed *in situ* during the co-crystallisation of the 37 kDa fragment and m<sub>3</sub>GpppG (Strasser *et al.*, 2004). Attempts to obtain the 26 kDa fragment either by preparative proteolysis or as recombinant protein failed, since this fragment precipitates due to unfolding or incorrect folding, respectively, in the absence of m<sub>3</sub>GpppG and is therefore not suitable for biochemical experiments. The *K*<sub>d</sub>-value for the m<sub>3</sub>GpppG dinucleotide (which is present in the crystal structure) was

determined to be 1.0 μM, while it is 12.1 μM for the m<sub>3</sub>GpppA dinucleotide. The crystal structure of the complex containing the m<sub>3</sub>GpppG dinucleotide reveals that the adenosine of m<sub>3</sub>GpppA could be harboured in the binding pocket as well, since there is no strong discrimination between the purines commonly caused by polar interactions. The higher *K*<sub>d</sub>-value of the m<sub>3</sub>GpppA appears to be related to the lack of two hydrogen bonds with Ser105. It turned out to be impossible to determine the exact *K*<sub>d</sub>-value of the m<sup>7</sup>GpppA dinucleotide by fluorescence spectroscopy, owing to an extremely large inner filter effect caused by the high dinucleotide concentrations required, but it can be estimated that the *K*<sub>d</sub>-value for m<sup>7</sup>GpppA is greater than 170 μM. Obviously, the difference in *K*<sub>d</sub>-values between m<sub>3</sub>GpppA and m<sup>7</sup>GpppA must be related to the two methyl groups on N2 of the m<sub>3</sub>G-base. These two methyl groups are in van der Waals (VDW) contact with Trp107, but the difference in affinities between m<sub>3</sub>GpppA/G and m<sup>7</sup>GpppA cannot be caused exclusively by the contribution of these two VDW contacts to the free binding energy. Hence, the difference in affinity should be related to the binding process itself. Upon binding to snurportin1 the cap is dehydrated, and hydrogen bonds to

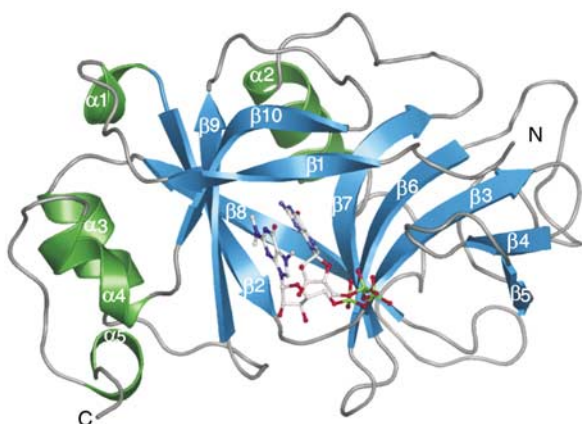


**Figure 1** Structure of human snurportin1 (residues 97–300) with bound m<sub>3</sub>GpppG-cap dinucleotide (PDB accession code 1XK5). Ribbon plot of the m<sub>3</sub>G-cap-binding domain with  $\beta$ -sheets coloured in blue,  $\alpha$ -helices in green and loop regions in grey. Secondary structure motifs are numbered consecutively from the N-terminus to the C-terminus. The m<sub>3</sub>GpppG dinucleotide is depicted in ball-and-stick mode with nitrogen atoms in blue, carbons in grey, oxygens in red and phosphorus atoms in green.

water molecules are replaced by hydrogen bonds to the protein. Obviously, the m<sup>7</sup>G- and m<sub>3</sub>G-caps differ in solution with respect to their hydration shells, as the m<sup>7</sup>G-cap is capable to bind two water molecules via its NH<sub>2</sub> group. These two water molecules have to be released for the binding of the m<sup>7</sup>G-cap requiring a substantial amount of energy, as these hydrogen bonds are not replaced by hydrogen bonds to the protein. The dimethylated N2 of the m<sub>3</sub>G-cap has no bound water molecules; hence its binding to snurportin1 and the hydrophobic interaction with the Trp107 side chain is much more favourable. These differences could already cause the observed differences in *K<sub>d</sub>*, but other molecular properties might additionally contribute to the discrimination.

The discrimination between m<sup>7</sup>G- and m<sub>3</sub>G-caps by snurportin1 might also be related to the strength of the cation- $\pi$  interaction. With respect to the p*K<sub>a</sub>*-value of 7.46 of m<sub>3</sub>GpppG (Wieczorek *et al*, 1995), the m<sub>3</sub>G-base is expected to be positively charged under crystallisation conditions (pH 5.5). As suggested for m<sup>7</sup>G-cap-binding proteins (Quiocho *et al*, 2000), a cation- $\pi$  interaction between the positively charged

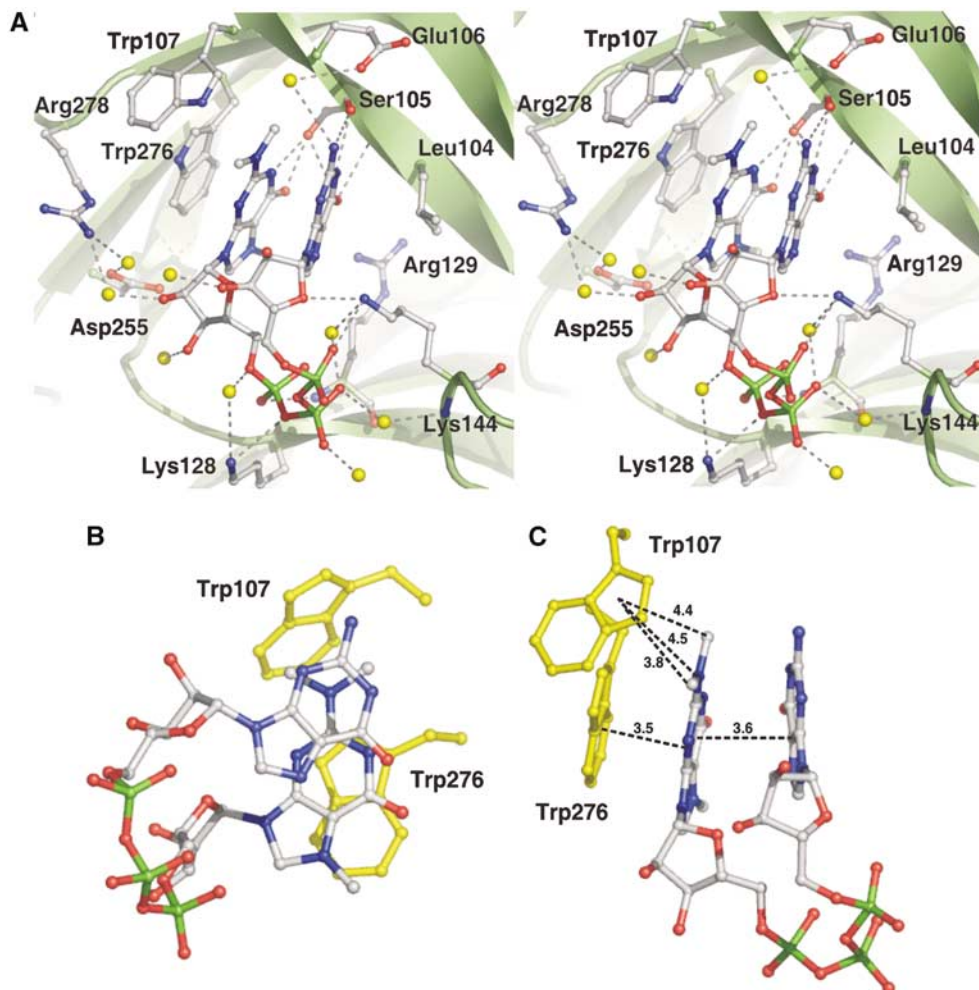


**Figure 2** The m<sub>3</sub>G-cap-binding pocket. Snurportin1 is shown in ribbon presentation and coloured in green. Side chains of residues interacting with the m<sub>3</sub>G-cap dinucleotide are shown in ball-and-stick mode. The m<sub>3</sub>G-cap dinucleotide is coloured as described in Figure 1. (A) Stereo view of the cap-binding pocket. Side chains forming hydrogen bonds or hydrophobic contacts with the cap are coloured as the m<sub>3</sub>G-cap, and water molecules involved in the interaction are shown as yellow balls. Hydrogen bonds are depicted as dashed grey lines. (B) Base stack of the m<sub>3</sub>GpppG dinucleotide, whereas Trp276 and Trp107 are coloured yellow. (C) Distances between both bases of the cap dinucleotide, between the m<sub>3</sub>G-base and Trp276 and between the atoms of the dimethylamine of the cap base and Trp107 are depicted as dashed black lines. Numbers indicate the distances in Å.

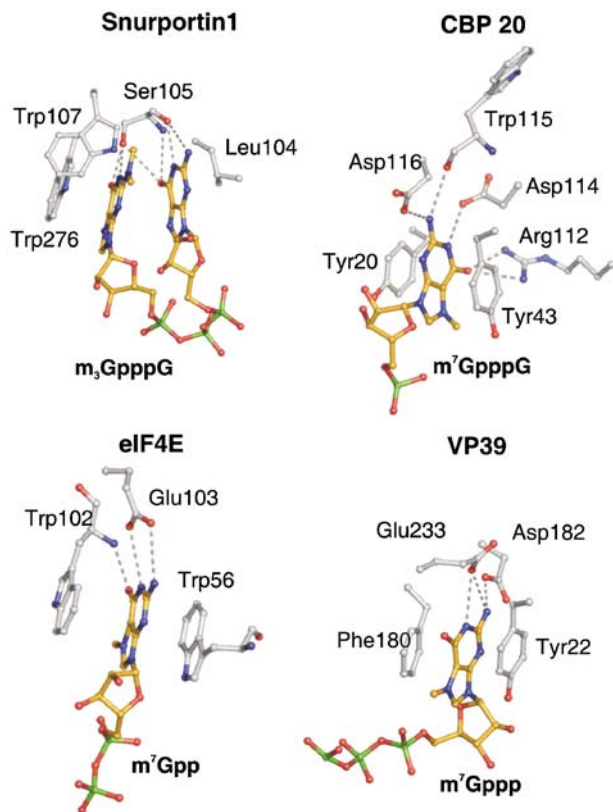


**Figure 3** Comparison of cap-binding pockets. m<sup>7</sup>G-cap-binding pockets of CBP20, eIF4E and the viral nucleoside 2'-O-methyltransferase (VP39) are presented in comparison to the m<sub>3</sub>G-cap-binding pocket of snurportin1. Side chains of residues interacting with the caps are depicted in ball-and-stick mode. Atoms of the caps and the interacting side chains are coloured as described in Figure 1, with the exception of carbon atoms of the dinucleotide, which are shown in orange. In all presented cases, the residues stacking the bases and those forming hydrogen bonds with the cap bases are depicted. Hydrogen bonds are shown as dashed grey lines.

**Table II** Binding constants of various m<sub>3</sub>G-cap oligoribonucleotides for human snurportin1

Cap oligo	K <sub>d</sub> values (μM)	Standard deviation of curve fit (μM)
m <sub>3</sub> GpppG	1.00 ± 0.03	0.12
m <sub>3</sub> GpppA	12.1 ± 0.55	2.72
m <sup>7</sup> GpppA	≥ 170 ± 12.9	17
m <sub>3</sub> GpppA <sub>m</sub> pU <sub>m</sub> pA	0.23 ± 0.02	0.08

trimethylated guanine and the coplanar aromatic side chain of Trp276 is expected. The presence of the two methyl groups bound to N2 probably changes the distribution of the positive charge within m<sub>3</sub>G in comparison to m<sup>7</sup>G and therefore significantly affects the cation–π interaction. Interestingly, Trp107 is only 4.5 Å distant to the N2 atom of the m<sub>3</sub>G-base (Figure 2C); hence, a cation–π interaction appears reasonable assuming a significant positive partial charge on N2 stabilised by the two methyl groups.

Consistent with a previous report (Huber *et al*, 1998), the binding of the synthetic tetranucleotide m<sub>3</sub>GpppA<sub>m</sub>pU<sub>m</sub>pA, which resembles more closely UsnRNAs *in vivo*, to full-length snurportin1 is even stronger (K<sub>d</sub> = 0.23 μM) than that of m<sub>3</sub>GpppG, which should be related to the presence of addi-

tional nucleotides and/or due to the 2'-O-methylated riboses. Inspection of the electrostatic surface potential of the m<sub>3</sub>G-cap-binding domain gives no hint on binding sites for the additional nucleotides (data not shown). However, the crystallised domain lacks the C-terminal 61 residues, which could extend the RNA-binding surface. To clarify the role of these C-terminal residues, the determination of the K<sub>d</sub>-value for the crystallised snurportin1 fragment would be necessary, but the 26 kDa fragment aggregates rapidly in the absence of m<sub>3</sub>GpppG (see above) and could therefore not be used for biochemical experiments.

The crystallised domain is also lacking the N-terminal 78 residues, raising the question whether the IBB domain could affect the m<sub>3</sub>G-cap-binding analogous to importin-α. This appears possible since the IBB domain of importin-α is known to compete with the NLS of a cargo for binding to importin-α (Kobe, 1999). To examine this potential autoinhibitory effect of the snurportin1 IBB domain on m<sub>3</sub>G-cap binding, the affinity of the m<sub>3</sub>GpppG was evaluated in the presence of increasing amounts of IBB domain (residues 1–65). Remarkably, even at 100-fold excess of IBB domain over snurportin1 (and a five-fold excess of m<sub>3</sub>GpppG over snurportin1) the affinity remains unaltered (see Supplementary Table 1a). In a second approach, an N-terminally truncated snurportin1 comprising residues 66–360 was used. The K<sub>d</sub>-value for m<sub>3</sub>GpppG turned out to be 1.24 μM (± 0.3 μM), which is close to the value of 1.0 μM (± 0.03 μM) observed for the full-length protein. Both experiments demonstrate that the IBB domain of snurportin1 does not exhibit an autoinhibitory effect on cargo binding as reported for importin-α.

### Role of tryptophan residues Trp276 and Trp107 in m<sub>3</sub>G-cap binding

An obvious feature of the m<sub>3</sub>G-cap-binding pocket is the presence of the two tryptophan residues Trp107 and Trp276 (Figure 2). In order to understand their functional significance, these tryptophan residues were substituted by alanine, either singly or together. The resulting mutated proteins were purified and characterised with regard to m<sub>3</sub>G-cap-binding affinity using fluorescence spectroscopy and an *in vitro* nuclear import assay. However, an exact determination of K<sub>d</sub>-values for the mutated proteins was not possible, as the strongly reduced affinities (see below) would require high concentrations of m<sub>3</sub>GpppG, leading to a very large internal filter effect. Therefore, the change in affinity was estimated comparing the changes in fluorescence upon addition of m<sub>3</sub>GpppG.

Binding of m<sub>3</sub>GpppG to wild-type snurportin1 leads to a decrease in fluorescence of 62.7% (± 3.9%), indicating a strong interaction. Taking the changed fluorescence properties of each mutant into account, the binding of m<sub>3</sub>GpppG decreases the fluorescence for the W276A and W107A mutants only by 20.0% (± 6.1%) and 25.0% (± 6.3%), respectively, and even less (15.8% (± 4.2%)) for the double mutant, corresponding to a reduced cap-binding activity. The effect of the W276A substitution is expected, as this tryptophan stacks on the m<sub>3</sub>G-base and forms a strong cation–π interaction. More interestingly, the W107A mutation shows almost the same reduction in fluorescence, suggesting an important role in m<sub>3</sub>G-cap binding. Since the two methyl groups of N2 are pointing towards Trp107, this tryptophan should have a substantial impact on the discrimination of m<sup>7</sup>G-cap-bearing

RNAs. Indeed, the binding affinity of m<sup>7</sup>GpppA to the W107A mutant is identical to that of m<sub>3</sub>GpppA, as determined by the decrease in tryptophan fluorescence (see Supplementary Table Ib). Hence, the fully solvent-exposed Trp107 plays an important role in the process of cap-binding and discrimination of m<sup>7</sup>G-caps.

Furthermore, the β-strand (β1) harbouring Trp107 exhibits a highly twisted conformation and might adopt a different, more relaxed conformation in the absence of the cap, with the side chain of Trp107 located inside the cap-binding pocket. However, there is currently no experimental evidence for such a conformational flexibility of the β-strand β1 or for an induced fold upon cap binding as observed for CBP20 (Calero *et al*, 2002; Mazza *et al*, 2002).

The essential role of these two tryptophan residues, Trp276 and Trp107, was also observed in the *in vitro* nuclear import assay using intact U1snRNPs as transport cargo. The decrease in import observed for the three mutants correlates quantitatively with the reduced cap-binding affinities evaluated by fluorescence spectroscopy (Figure 4). Therefore, it appears unlikely that snurportin1 forms other strong contacts, like protein-protein interactions, with the U1snRNP. However, the nuclear import of UsnRNPs *in vivo* was reported to occur by means of a larger complex containing snurportin1, importin-β, the SMN protein and presumably other components of the SMN complex (Narayanan *et al*, 2002, 2004).

### Structural homology

Searching the PDB for structurally related proteins revealed that the overall fold of the m<sub>3</sub>G-cap-binding domain exhibits high structural similarity to the GTP-binding domain of the

mRNA-guanylyltransferase indicated by an r.m.s.d. of 2.6 Å for 204 common C<sub>α</sub> atoms. Interestingly, this enzyme is involved in the formation of the 5'-cap as it transfers GMP to the 5' end of mRNAs and UsnRNAs via a 5'-5'-triphosphate bridge (Hakansson *et al*, 1997). This domain is also found in DNA ligases, where it is involved in ATP binding (Subramanya *et al*, 1996). Superposing the structures of snurportin1 and mRNA-guanylyltransferase, which shares the highest structural similarity to snurportin1, reveals that the binding sites for GTP and the m<sub>3</sub>G-cap are in a similar area of the protein surface, but the positions of the nucleotides and the residues forming the binding pocket, and therefore all interactions, are completely different (Figure 5A/B). Furthermore, the GTP-binding pocket of the mRNA-guanylyltransferase penetrates much more deeply between the β-sheets than the m<sub>3</sub>G-cap-binding pocket of snurportin1.

The structural homology between the m<sub>3</sub>G-cap-binding domain and the mRNA-guanylyltransferase was unexpected, since all searches for sequences homologous to the m<sub>3</sub>G-cap-binding domain gave no significant hint to any other protein (Huber *et al*, 1998). Indeed, the amino-acid sequence identity between the human m<sub>3</sub>G-cap-binding domain and the human mRNA-guanylyltransferase is only 12.7% (Figure 5C). A more elaborate database search recently identified the m<sub>3</sub>G-cap-binding domain of snurportin1 as an inactive paralogue of the mRNA-guanylyltransferase (Mans *et al*, 2004). The structural homology suggests that the m<sub>3</sub>G-cap-binding domain shares a common ancestor with the GTP-binding domain of the mRNA-guanylyltransferase that was linked to an IBB domain by shuffling and fusion of the corresponding exons.

## Materials and methods

### Structure determination

Purification, m<sub>3</sub>G-cap-binding affinity test and crystallisation strategy are described elsewhere (Strasser *et al*, 2004). Shortly, crystals of a 26 kDa m<sub>3</sub>G-cap-binding domain of snurportin1 were only obtained in the presence of the synthetic m<sub>3</sub>GpppG-cap dinucleotide. Single crystals for X-ray data collection were grown in sitting drops using 8–10% (w/v) PEG 10k and 200 mM sodium citrate (pH 5.5) as precipitant. Diffraction data of a native crystal were collected at the PSF beamline BL1 (BESSY, Berlin) to a resolution of 2.4 Å. Three different heavy-atom derivative data sets were collected on a Micromax 007 rotating anode generator (Rigaku/MSO, USA) operating at 40 kV and 20 mA, equipped with Osmic focusing mirrors and a Mar345dtb detector system (Xray-Research, Germany) in order to solve the phase problem. Data were processed using Denzo/Scalepack (HKL-research) and CCP4 programs (Bailey, 1994). Heavy-atom sites were found and initial phases were improved by AutoSHARP (Globalphasing Ltd, UK). The graphics program O (Jones *et al*, 1991) was used for model-building and the structure was refined with CNS (Brünger *et al*, 1998). A 37 kDa fragment of snurportin1 was used for crystallisation, but the crystals contain only a 26 kDa fragment. Inspection of possible GluC-protease cleavage sites and preliminary mass spectroscopic data indicates that this fragment consists of residues 79–300. The refined model comprises residues 97–300. The missing residues are not defined in the electron density map due to conformational flexibility. The m<sub>3</sub>GpppG-cap dinucleotide was well defined in the electron density map.

Topology and parameter files for the m<sub>3</sub>GpppG-cap dinucleotide were created with the help of the Dundee PRODRG2 Server (van Aalten *et al*, 1996). Secondary structure elements were assigned by STRIDE (Frishman and Argos, 1995) and figures were generated with Pymol (www.pymol.org).

### Expression constructs

For all expression constructs described, full-length snurportin1 in pGEX6P1 (Amersham Biosciences) was used as a PCR template

	DAPI	U1snRNP	Fluorescence intensity (a.u.)	Import activity (%)
-SPN1wt			—	—
+SPN1wt			42 (±7)	100
+SPN1W276A			6 (±3)	14
+SPN1W107A			11 (±3)	26
+SPN1W276/107A			5 (±4)	12

**Figure 4** *In vitro* nuclear import assay of snurportin1. Nuclear import of fluorescently labelled U1snRNPs in the presence of importin-β, RanGDP, NTF2, an energy regenerating system, and either snurportin1 or one of the mutated proteins (W107A, W276A, and W107A/W276A). In the left panel, cell nuclei stained with DAPI are shown. The middle panel shows the import of Cy3-labelled U1snRNPs. The quantification of the import rates is given in the right panel (a.u.: arbitrary units for intensity per pixel).

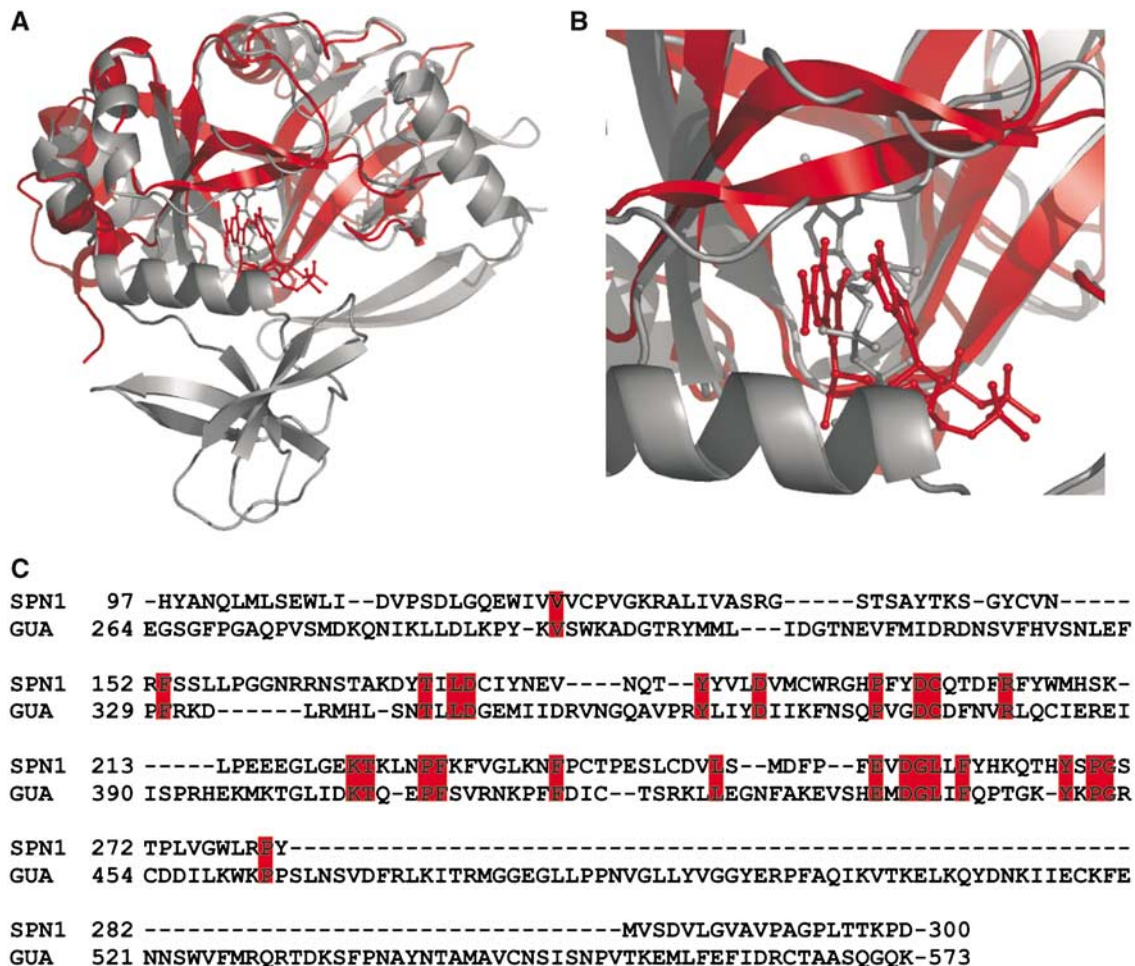


**Figure 5** Structural similarity of snurportin1 with bound m<sub>3</sub>GpppG to the mRNA-guanylyltransferase with bound GTP. (A) Superimposed protein structures presented as ribbon diagrams and the bound nucleotides in ball-and-stick representation. Human snurportin1–m<sub>3</sub>GpppG complex (coloured red) and the mRNA-guanylyltransferase–GTP complex (coloured grey) of the *Paramecium bursaria* chlorella virus 1 (PDB accession code 1CKM) share an amino-acid sequence identity of 8.3% for the structurally homologous regions. (B) Close-up view of the nucleotide-binding pockets. In the mRNA-guanylyltransferase, the bound GTP protrudes much deeper into the cleft between the  $\beta$ -sheets. (C) Structure-based sequence alignment of human snurportin1 and human mRNA-guanylyltransferase reveals a sequence identity of 12.7%.

(Strasser *et al*, 2004). The coding region of the deletion mutant of snurportin1 (residues 66–360) was amplified using primers with restriction sites for *Bam*HI and *Xho*I and inserted into pGEX6P1. The IBB domain (residues 1–65) was cloned in pET28b (Novagen) via *Nco*I and *Xho*I restriction sites. Tryptophan mutants W276A, W107A and W276A/W107A in pGEX6P1 were generated using the QuickChange™ Site Directed Mutagenesis Kit (Stratagene).

#### Protein expression and purification

Expression and purification of snurportin1 wild-type, truncated snurportin1 (residues 66–360) and the tryptophan mutants were performed as described previously (Strasser *et al*, 2004). The IBB domain (residues 1–65) was expressed as a His-tagged protein at 30°C for 5 h using 1 mM IPTG and purified at first by Ni-NTA agarose. Therefore, the supernatant was applied to the resin in 300 mM NaCl, 20 mM Tris, pH 7.5, 2 mM 2-mercaptoethanol, and eluted with the loading buffer containing 300 mM imidazole. The fractions containing the IBB domain were pooled, concentrated and further purified by gel filtration on Superdex 75 media (100 mM NaCl, 50 mM HEPES, pH 7.5, 2 mM DTT).

#### Fluorescence spectroscopy

Fluorescence measurements were performed on a Fluoromax3™ spectrofluorimeter (Jobin Yvon) at 20°C in 100 mM NaCl, 50 mM HEPES/NaOH (pH 7.5), using cuvettes with 0.5 × 1.0 cm<sup>2</sup> section (Hellma). Emission at 315 or 340 nm, used for the calculation of dissociation constants, was recorded during excitation at 295 nm

(1 nm bandwidth) for 60 s with time constants of 0.5 s. Equilibrium dissociation constants were obtained by fitting the solutions of a quadratic function, assuming a 1:1 stoichiometry and taking into account the fluorescence of the cap oligonucleotides (Graphit 3.1, Erithacus Software). Standard deviations were calculated from three independent experiments. To determine the cap-binding affinity of wild-type snurportin1 and of the mutants W107A, W276A and W107A/W276A, emission spectra (310–500 nm) were collected after excitation at 295 nm for the proteins alone and in the presence of m<sub>3</sub>GpppG in a 20-fold, or in case of m<sup>7</sup>GpppA and m<sub>3</sub>GpppA in a 50-fold, molar excess. Spectra were corrected for the fluorescence of the cap dinucleotides and buffer contributions. The decrease in fluorescence upon ligand binding to snurportin1 was determined in three independent measurements. For competition experiments with the IBB domain, the decrease in tryptophan fluorescence after addition of m<sub>3</sub>GpppG in a five-fold molar excess to snurportin1 full length was compared to the decrease after addition of increasing amounts of the IBB domain (residues 1–65). The IBB domain was titrated up to a 100-fold molar excess to snurportin1 wild type.

#### Nuclear import assay

Nuclear import assays were performed as described by Huber *et al* (2002). Each transport reaction mixture contained 100 nM Cy3-labelled human U1snRNPs, and, except for the negative control, 500 nM importin- $\beta$ , 300 nM of snurportin1 or the mutated snurportin1 proteins (W107A, W276A and W107A/W276A). The transport was performed on permeabilised HeLa cells for 10 min

at room temperature in a humidified chamber. After extensive washing with 1 × PBS, the cells were fixed with paraformaldehyde (5% in 1 × PBS) and mounted on coverslips. Images were taken at 400-fold magnification. Rates of U1snRNP import were calculated with the help of the program ImageJ (<http://rsb.info.nih.gov/ij/>), by averaging nuclear fluorescence intensities of 50 cells. In order to compare the results, the intensities of each experiment were normalised against wild-type snurportin1 intensities.

### Supplementary data

Supplementary data are available at *The EMBO Journal* Online.

## References

- Bailey S (1994) The CCP4 Suite—programs for protein crystallography. *Acta Crystallogr D* **50**: 760–763
- Brünger AT, Adams PD, Clore GM, DeLano WL, Gros P, Grosse-Kunstleve RW, Jiang JS, Kuszewski J, Nilges M, Pannu NS, Read RJ, Rice LM, Simonson T, Warren GL (1998) Crystallography & NMR system: a new software suite for macromolecular structure determination. *Acta Crystallogr D* **54**: 905–921
- Calero G, Wilson KF, Ly T, Rios-Steiner JL, Clardy JC, Cerione RA (2002) Structural basis of m<sup>7</sup>GpppG binding to the nuclear cap-binding protein complex. *Nat Struct Biol* **9**: 912–917
- Chook YM, Blobel G (2001) Karyopherins and nuclear import. *Curr Opin Struct Biol* **11**: 703–715
- Fischer U, Darzynkiewicz E, Tahara SM, Dathan NA, Lührmann R, Mattaj IW (1991) Diversity in the signals required for nuclear accumulation of U snRNPs and variety in the pathways of nuclear transport. *J Cell Biol* **113**: 705–714
- Fischer U, Lührmann R (1990) An essential signaling role for the m<sup>3</sup>G cap in the transport of U1 snRNP to the nucleus. *Science* **249**: 786–790
- Fischer U, Sumpster V, Sekine M, Satoh T, Lührmann R (1993) Nucleo-cytoplasmic transport of U snRNPs: definition of a nuclear location signal in the Sm core domain that binds a transport receptor independently of the m<sup>3</sup>G cap. *EMBO J* **12**: 573–583
- Frishman D, Argos P (1995) Knowledge-based protein secondary structure assignment. *Proteins* **23**: 566–579
- Görlich D, Henklein P, Laskey RA, Hartmann E (1996) A 41 amino acid motif in importin- $\alpha$  confers binding to importin- $\beta$  and hence transit into the nucleus. *EMBO J* **15**: 1810–1817
- Görlich D, Kutay U (1999) Transport between the cell nucleus and the cytoplasm. *Annu Rev Cell Dev Biol* **15**: 607–660
- Gubitz AK, Feng W, Dreyfuss G (2004) The SMN complex. *Exp Cell Res* **296**: 51–56
- Hakansson K, Doherty A, Shuman S, Wigley D (1997) X-ray crystallography reveals a large conformational change during guanyl transfer by mRNA capping enzymes. *Cell* **89**: 545–553
- Hodel AE, Gershon PD, Quijcho FA (1998) Structural basis for sequence-nonspecific recognition of 5'-capped mRNA by a cap-modifying enzyme. *Mol Cells* **1**: 443–447
- Hodel AE, Gershon PD, Shi X, Wang SM, Quijcho FA (1997) Specific protein recognition of an mRNA cap through its alkylated base. *Nat Struct Biol* **4**: 350–354
- Hu G, Oguro A, Li C, Gershon PD, Quijcho FA (2002) The 'cap-binding slot' of an mRNA cap-binding protein: quantitative effects of aromatic side chain choice in the double-stacking sandwich with cap. *Biochemistry* **41**: 7677–7687
- Huber J, Cronshagen U, Kadokura M, Marshallsay C, Wada T, Sekine M, Lührmann R (1998) Snurportin1, an m<sup>3</sup>G-cap-specific nuclear import receptor with a novel domain structure. *EMBO J* **17**: 4114–4126
- Huber J, Dickmanns A, Lührmann R (2002) The importin- $\beta$  binding domain of snurportin1 is responsible for the Ran- and energy-independent nuclear import of spliceosomal U snRNPs *in vitro*. *J Cell Biol* **156**: 467–479
- Jones TA, Zou JY, Cowan SW, Kjeldgaard M (1991) Improved methods for building protein models in electron density maps and the location of errors in these models. *Acta Crystallogr A* **47**: 110–119
- Jullien D, Görlich D, Laemmli UK, Adachi Y (1999) Nuclear import of RPA in *Xenopus* egg extracts requires a novel protein XRP1 $\alpha$  but not importin  $\alpha$ . *EMBO J* **18**: 4348–4358
- Kobe B (1999) Autoinhibition by an internal nuclear localization signal revealed by the crystal structure of mammalian importin  $\alpha$ . *Nat Struct Biol* **6**: 388–397
- Mans BJ, Anantharaman V, Aravind L, Koonin EV (2004) Comparative genomics, evolution and origins of the nuclear envelope and nuclear pore complex. *Cell Cycle* **3**: e99–e123
- Marcotrigiano J, Gingras AC, Sonenberg N, Burley SK (1997) Crystal structure of the messenger RNA 5' cap-binding protein (eIF4E) bound to 7-methyl-GDP. *Cell* **89**: 951–961
- Massenet S, Pellizzoni L, Paushkin S, Mattaj IW, Dreyfuss G (2002) The SMN complex is associated with snRNPs throughout their cytoplasmic assembly pathway. *Mol Cell Biol* **22**: 6533–6541
- Matsuo H, Li H, McGuire AM, Fletcher CM, Gingras AC, Sonenberg N, Wagner G (1997) Structure of translation factor eIF4E bound to m<sup>7</sup>GDP and interaction with 4E-binding protein. *Nat Struct Biol* **4**: 717–724
- Mattaj IW (1986) Cap trimethylation of U snRNA is cytoplasmic and dependent on U snRNP protein binding. *Cell* **46**: 905–911
- Mazza C, Segref A, Mattaj IW, Cusack S (2002) Large-scale induced fit recognition of an m<sup>7</sup>GpppG cap analogue by the human nuclear cap-binding complex. *EMBO J* **21**: 5548–5557
- Meister G, Eggert C, Fischer U (2002) SMN-mediated assembly of RNPs: a complex story. *Trends Cell Biol* **12**: 472–478
- Mouaikel J, Verheggen C, Bertrand E, Tazi J, Bordonne R (2002) Hypermethylation of the cap structure of both yeast snRNAs and snoRNAs requires a conserved methyltransferase that is localized to the nucleolus. *Mol Cells* **9**: 891–901
- Narayanan U, Achsel T, Lührmann R, Matera AG (2004) Coupled *in vitro* import of U snRNPs and SMN, the spinal muscular atrophy protein. *Mol Cells* **16**: 223–234
- Narayanan U, Ospina JK, Frey MR, Hebert MD, Matera A (2002) SMN, the spinal muscular atrophy protein, forms a pre-import snRNP complex with snurportin1 and importin  $\beta$ . *Hum Mol Genet* **11**: 1785–1795
- Niedzwiecka A, Marcotrigiano J, Stepinski J, Jankowska-Anyszka M, Wyslouch-Cieszyńska A, Dadlez M, Gingras AC, Mak P, Darzynkiewicz E, Sonenberg N, Burley SK, Stolarski R (2002) Biophysical studies of eIF4E cap-binding protein: recognition of mRNA 5' cap structure and synthetic fragments of eIF4G and 4E-BP1 proteins. *J Mol Biol* **319**: 615–635
- Ohno M, Segref A, Bachi A, Wilm M, Mattaj IW (2000) PHAX, a mediator of U snRNA nuclear export whose activity is regulated by phosphorylation. *Cell* **101**: 187–198
- Palacios I, Hetzer M, Adam SA, Mattaj IW (1997) Nuclear import of U snRNPs requires importin  $\beta$ . *EMBO J* **16**: 6783–6792
- Plessel G, Fischer U, Lührmann R (1994) m<sup>3</sup>G cap hypermethylation of U1 small nuclear ribonucleoprotein (snRNP) *in vitro*: evidence that the U1 small nuclear RNA-(guanosine-N<sub>2</sub>)-methyltransferase is a non-snRNP cytoplasmic protein that requires a binding site on the Sm core domain. *Mol Cell Biol* **14**: 4160–4172
- Quijcho FA, Hu G, Gershon PD (2000) Structural basis of mRNA cap recognition by proteins. *Curr Opin Struct Biol* **10**: 78–86
- Raker VA, Plessel G, Lührmann R (1996) The snRNP core assembly pathway: identification of stable core protein heteromeric complexes and an snRNP subcore particle *in vitro*. *EMBO J* **15**: 2256–2269
- Segref A, Mattaj IW, Ohno M (2001) The evolutionarily conserved region of the U snRNA export mediator PHAX is a novel RNA-binding domain that is essential for U snRNA export. *RNA* **7**: 351–360
- Strasser A, Dickmanns A, Schmidt U, Penka E, Urlaub H, Sekine M, Lührmann R, Ficner R (2004) Purification, crystallization

## Acknowledgements

We thank the staff of PSF beamline BL1 at BESSY (Berlin) for excellent support during data collection. We are grateful to our colleague Markus Rudolph for help with fluorescence spectroscopy experiments and to Jörg Kahle and Detlef Doenecke for the opportunity to perform nuclear import assays. We thank M Sekine for providing a synthetic m<sup>3</sup>G-cap-tetranucleotide. This work was supported by the Deutsche Forschungsgemeinschaft (SFB523). The coordinates and structure factors have been deposited in the Protein Data Base (PDB accession code 1XK5).



- and preliminary crystallographic data of the m<sup>3</sup>G cap-binding domain of human snRNP import factor snurportin 1. *Acta Crystallogr D* **60**: 1628–1631
- Subramanya HS, Doherty AJ, Ashford SR, Wigley DB (1996) Crystal structure of an ATP-dependent DNA ligase from bacteriophage T7. *Cell* **85**: 607–615
- Tomoo K, Shen X, Okabe K, Nozoe Y, Fukuhara S, Morino S, Sasaki M, Taniguchi T, Miyagawa H, Kitamura K, Miura K, Ishida T (2003) Structural features of human initiation factor 4E, studied by X-ray crystal analyses and molecular dynamics simulations. *J Mol Biol* **328**: 365–383
- van Aalten DM, Bywater R, Findlay JB, Hendlich M, Hoof RW, Vriend G (1996) PRODRG, a program for generating molecular topologies and unique molecular descriptors from coordinates of small molecules. *J Comput Aided Mol Des* **10**: 255–262
- Weis K (2003) Regulating access to the genome: nucleocytoplasmic transport throughout the cell cycle. *Cell* **112**: 441–451
- Wieczorek Z, Stepinski J, Jankowska M, Lönnberg H (1995) Fluorescence and absorption spectroscopic properties of RNA 5'-cap analogues derived from 7-methyl-, N<sup>2</sup>, 7-dimethyl- and N<sup>2</sup>, N<sup>2</sup>, 7-trimethyl-guanosines. *J Photochem Photobiol* **28**: 57–63
- Will CL, Lührmann R (2001) Spliceosomal UsnRNP biogenesis, structure and function. *Curr Opin Cell Biol* **13**: 290–301
- Yong J, Wan L, Dreyfuss G (2004) Why do cells need an assembly machine for RNA-protein complexes? *Trends Cell Biol* **14**: 226–232